Electrochemistry Communications 158 (2024) 107644

Contents lists available at ScienceDirect

Electrochemistry Communications

journal homepage: www.elsevier.com/locate/elecom

$LiNi_{1/3}Mn_{1/3}Co_{1/3}O_2$/graphite cells adopting polyolefin and non-polyolefin separators for potential application in industrial manufacturing of energy storage devices

Louis Hamenu [a,*], Latifatu Mohammed [b], Juliet Attah [c], Rafia Abdul-Samii [b,d], Eric Nyarko [b,e], Anna Monney Hammond [b], Godfred Ofotsu Tottimeh [b,f], Joyce Koranteng [b,g], Kennedy Andoh [b], Alfred Madzvamuse [h]

[a] Department of Chemistry, School of Physical and Mathematical Sciences, College of Basic and Applied Sciences University of Ghana, Legon, Ghana
[b] Institute of Industrial Research, Council for Scientific and Industrial Research, P. O. Box LG 576, 92 Boundary Road, East Legon, Ghana
[c] Nuclear Chemistry and Environmental Research Centre, National Nuclear Research Institute, Ghana Atomic Energy Commission, Kwabenya-Accra, Ghana
[d] Institute for Environment and Sanitation Studies, IESS, University of Ghana, Box 209, Legon, Accra, Ghana
[e] Department of Renewable Energy Engineering, University of Energy and Natural Resources Sunyani, Ghana
[f] Department of Chemical Engineering, Kwame Nkrumah University of Science and Technology, Kumasi, Ghana
[g] Department of Materials Science & Engineering, University of Ghana, Annie Jiaggie Road, Legon-Accra, Ghana
[h] Department of Chemistry, University of Zimbabwe, P. O. MP 167, Mount Pleasant, Harare, Zimbabwe

ARTICLE INFO

Keywords:
Separator membranes
Nonwoven
Polyolefin
Lithium-ion-battery
Physical properties
Electrochemical property

ABSTRACT

This study features comprehensive physical and electrochemical properties of different polyolefin and non-polyolefin separators. These separators include polypropylene-polyethylene-polypropylene (PEP), polyethylene (PE), Al_2O_3-coated polypropylene (C-PP), polyethylene terephthalate (PET), and Silicon carbide mat (SiCmat). The interaction of the different separators and the electrolyte was investigated in terms of ionic conductivity, contact angle test, electrolyte uptake, and electrolyte oxidation. The full cells fabricated using the different separators were also studied for charge–discharge performance, cycle performance, and internal resistance. Results showed that the different separators demonstrated different physical and electrochemical behavior. The non-polyolefin separators registered a small electrolyte contact angle due to their high porosity and structural compatibility with the electrolyte. At 10 C-Rate, the specific capacity is in the order of PET > SiCmat > C-PP > PE > PEP corresponding to 90 mAh/g, 85 mAh/g, 70 mAh/g, 60 mAh/g and 40 mAh/g respectively. After 100 cycles at 1.0 C-rate, the cycle performance is in the order of PE > PET > C-PP > SiCmat > PEP corresponding to 70 %, 65 %, 61 %, 51 % and 49 % respectively. Thermally, PET, C-PP and SiCmat showed better thermal stability compared to the other separators. Therefore, Industrial production that requires high thermal stability may rely on C-PP, PET, or SiCmat, while PET and SiCmat offer better cycle performance and may replace commercially available PE and PEP.

1. Introduction

Lithium-ion battery (LIB) technology has attracted a lot of attention among secondary batteries due to its promising usage in electric vehicles and power grids as a clean energy source [1,2]. The past decade has seen a shift in the application of lithium-ion batteries from common consumer electronics to sophisticated applications including the locomotive industry. In the automobile industry today, LIB technology has been used as an electrification system for vehicles including hybrid vehicles, plug-in hybrid electric vehicles and fully electric vehicles [3,4]. The pursuit to enhance the electrification and performance derived from LIB has stimulated myriad publications concentrating on cathode materials with either high specific capacity or high potential window, and therefore higher energy density [5]. Among the cathode active materials investigated so far, nickel-rich layered structured materials ($LiNi_xCo_yMn_zO_2$) have been discovered to pragmatically find unquestionable applications in the locomotive industry for the next decade [6]. These cathodes with layered structures have attracted extreme attention as a

* Corresponding author.
E-mail address: Latifatu.mohammed@yahoo.com (L. Mohammed).

https://doi.org/10.1016/j.elecom.2023.107644
Received 23 October 2023; Received in revised form 25 November 2023; Accepted 1 December 2023
Available online 3 December 2023

result of their superior electrochemical property and structural stability comparable to the conventional $LiCoO_2$ [7,8].

The separator just like the cathode, anode and electrolyte plays an important role in the lithium-ion battery cell performance. The separator partitions the anode from the cathode aiding charge separation between the two electrodes. The movement of lithium ions in and out of the anode and the cathode is accompanied by the movement of electrons through the external circuit. During discharge, the electric current generated in the external circuit powers the load. The separator additionally holds the liquid electrolyte between the anode and the cathode [9]. To maintain the long operational performance of the cell, a standard separator should be robust, chemically and electrochemically inert, thermally stable and affordable. The tailored separator in addition should be thin, porous and easily wet by the electrolyte solvent to allow for easy diffusion of ions across its membrane. Battery separators can be grouped into nonwoven separators, microporous separators, electrospun separators, surface-modified separators, polymer blended separators and composite separators depending on the composition, structure and associated properties of the separator. A summary of the diverse types of separators employed in lithium-ion batteries is shown in Fig. 1. The commercial microporous separators for batteries are made from polyolefins. Although polyolefin separators are robust they have poor electrolyte-wetting properties and poor thermal stability [10]. These undesirable properties of polyolefins have been improved in many ways by chemical treatment, polymer grafting, plasma treatment and surface coating of the membranes with ceramic materials [11–15]. In certain cases, polymer blends have been used as separators to offer structural integrity and to enhance electrolyte adsorption [16]. Also, fabrication processes such as melt blow [17], air and wet-lay [18], and melt and electrospinning [19] have been introduced to increase the fiber content and porosity of some separators to make them high-performing [20]. Carlos et al. summarized the different works done on different types of separators employed in lithium-ion batteries [21]. In their review, they discussed the materials used, the method of separator preparation, the electrolyte employed, the ionic conductivity of the separator and the capacity obtained for the different separators and concluded the nonwoven separators as the best contender for the lithium-ion battery [21]. In other literature, the electrospinning process was observed to produce separators with large surface areas, high porosity and well-developed interconnected pores [22]. This makes electrospun separators superior in terms of their mechanical strength, wettability and electrolyte uptake which are highly recommended for the lithium-ion battery [22].

Regardless of the number of publications on the different types of separators fabricated for lithium-ion batteries, the comparative effect of these separators on the electrochemical behavior of LIBs containing nickel-rich cathode materials to the best of our knowledge is inadequate. This kind of investigation is crucial for guiding in obtaining an ideal system for LIB for industrial manufacturing and applications such as electric vehicles.

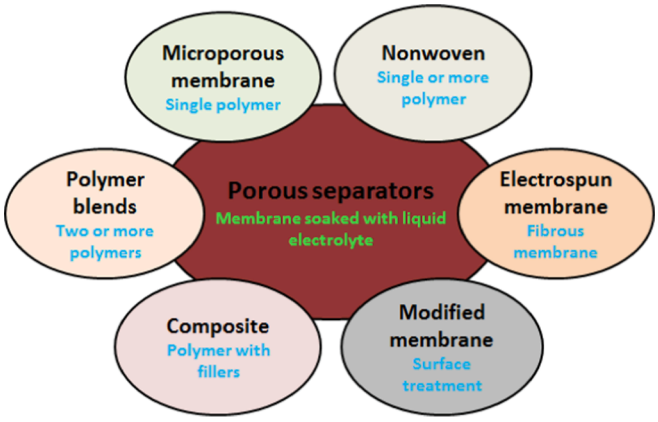

Fig. 1. Various type of separator materials for Lithium-ion battery.

In this work, the impact of the physicochemical properties of different separators on the electrochemical performance of $LiNi_{1/3}Mn_{1/3}Co_{1/3}O_2$/separator/graphite cells in a non-aqueous electrolyte is comparatively studied. The different separators consisting of microporous polyolefin separators (polyethylene (PE) and polypropylene-polyethylene-polypropylene (PEP)), Al_2O_3-coated polypropylene (C-PP), nonwoven separators (Silicon carbide mat (SiCmat), and polyethylene terephthalate (PET)) where employed in this study.

2. Experimental

2.1. Materials

$LiNi_{1/3}Mn_{1/3}Co_{1/3}O_2$ and Graphite (20 μm, SCMG-AR) were supplied by Ecopro, Korea and Showa Denko, Japan. 1 M $LiPF_6$ (EC/DMC = 3:7) was purchased from PANAX ETEC, Korea. Super P was sourced from Imerys, Switzerland. Polyvinylidene fluoride (PVDF, Kreha, Japan, Mw = 350,000) and N-methyl-2-pyrrolidone (NMP 99 wt%, Sigma Aldrich) as dispersing agents. Polypropylene-polyethylene-polypropylene (PEP), Polyethylene (PE), and Al_2O_3-coated polypropylene (C-PP) were purchased from Celgard. Polyethylene terephthalate (PET) and Silicon carbide (SiC) mat separators were donated by Kokam Company, South Korea.

2.2. Separator characterization

A high-resolution SU5000 (HITACHI, Japan) Field Emission Scanning Electron Microscope (FESEM) operated at 2.0 KV was employed to probe the morphology of the various separators. The thermal stability of the different separators was evaluated employing a Thermtest TGA-n 1000 thermal analyzer (Thermtest Instruments, USA) equipped with the Infinity Pro Thermal Analysis software. 3.45 mg of the samples were placed in an alumina (Al_2O_3) crucible (50 mg capacity), A temperature range between 25 °C and 800 °C at a rising rate of 10 °C/min and a cooling rate of 50 °C/min in nitrogen atmosphere was applied. The thermal shrinking test was done by heating the different separators in an oven at 140 °C temperature over 3 h. The membrane thickness was determined using a digital micrometer (Model: ID-C112BS). The wettability property of the different separators was determined by electrolyte contact angle measurements. 1 M $LiPF_6$ (EC/DMC = 3:7) electrolyte solution was dropped onto the separators and the established contact angles between the electrolyte and the separators were measured using a contact angle analyzer (SEO, Phoenix 150, Korea). The uptake of 1 M $LiPF_6$ (EC/DMC = 3:7) electrolyte by the separators was estimated using Equation (1). To do this the dry mass (W_o) of the separators was measured. After the separators were immersed in the electrolyte solution for 48 h, the excess electrolyte on the separator surface was wiped off with filter paper. The wet mass of the separators was recorded as W_t.

$$\text{Electrolyte uptake} = \frac{W_t - W_o}{W_t} \times 100 \quad (1)$$

2.3. Electrochemical characterization of separators

Complex impedance spectroscopy was used to determine the resistivity of the various separators soaked with the 1 M $LiPF_6$ (EC/DMC = 3:7) (v/v) on Autolab workstation (PGstat 100, Eco Chemie, Netherlands) in a frequency range of 1 MHz − 0.01 Hz. The various separators soaked in the electrolyte were sandwiched between two nickel electrodes (1 cm x 1 cm) in an Al-pouch. The resistivity in the separators soaked with the 1 M $LiPF_6$ (EC/DMC = 3:7) electrolyte was estimated according to the Equation (2)

$$\rho = \frac{R_s \times S}{d} \quad (2)$$

Where Rs is the solution resistance obtained from the Nyquist plot real axis in the high-frequency region, d is the thickness of the separator between the two electrodes, and S is the area of the electrodes.

The electrochemical stability window of the different separators was determined using linear sweep voltammetry (LSV). LSV was run on a coin-type (2032) half cells consisting of stainless steel plates as working electrodes, lithium metal foil as counter and reference electrodes, liquid electrolyte and the different separator on an Autolab instrument (ECO CHEMIE PGSTAT 100) in a potential window of 2 – 6 V at a scan rate of 0.1 mV/s.

2.4. Cathode and anode fabrication

$LiNi_{1/3}Mn_{1/3}Co_{1/3}O_2$ (NCM-333) cathode was prepared by casting a slurry consisting of 94 % NCM-333 (NCM-070, 10 μm, Ecopro, Korea) as active material, 3 wt% Super-P as a conductive additive, 3 wt% polyvinylidene fluoride (PVDF, Kreha, Japan, Mw = 350,000) as a binding agent in N-methyl-2-pyrrolidone (NMP, Sigma Aldrich) as a dispersing agent. The viscous slurry was cast on an aluminum foil (15 μm, San-A Aluminum, Korea) via a doctor blade apparatus. The coated slurry was dried at 120 °C for 2 h and then pressed with a roll pressing machine (WV-60, Samyang 60, South Korea). The electrodes were punched into a spherical disc with a diameter of 14 mm. The thickness and the loading concentration of the electrodes were 42 μm and 13.0 $mgcm^{-2}$ respectively. The positive electrode comprises 87 wt% natural graphite as the active material, 7 wt% PVDF and 5 wt% Super-P was coated on copper foil (10 μm, Iljin materials, Korea). The cast slurry was dried at 100 °C for 2 h, pressed and punched into a spherical disk with a diameter of 16 mm. The thickness and loading concentration were adjusted to 35 μm and 5.2 mg respectively.

2.5. Full cell-type preparation and electrochemical investigation

Full cells were assembled as CR2032-type coin cells by sandwiching the various separators between the cathode (NCM-333) and the anodes (natural graphite) in an argon-filled glove box. The constructed full cells with the various separators were aged for 24 h and then cycled at constant current (CC) mode for charging and CC mode for discharging at a C-rate of 0.1C in a voltage range of 2.8 V – 4.6 V using a cycler (Toscat 3000, Toyo systems). Subsequently, the cells were charged at a constant current/constant voltage (CC/CV) mode at 0.1C-rate and discharged at CC mode at different C-rate (0.1C – 10), in the voltage range of 2.8 V – 4.6 V. Electrochemical impedance spectroscopy was used to measure the total resistance of the cells in a frequency range of 0.01 Hz to 1 MHz at open circuit potential (OCP). The cells were cycled 100 times at 1.0C, between 2.8 V and 4.6 V to ascertain the stability of the cells.

3. Results and discussion

The morphological properties of the separators were evaluated using SEM. The SEM images in Fig. 2 (a-e) of the separators provide information for the comparison of separator porosities summarized in Fig. 2f. The porosities of the polyolefin (polypropylene-polyethylene-polypropylene (PEP) and polyethylene (PE)) separators are comparable. The polyolefin separators have relatively finer and uniform fibers as visualized in the SEM images in Fig. 2a and Fig. 2c. In PEP and PE separators, the cross-network of fine fibers form a membrane with uniform pore structure and pore size distribution. A porosity value of 42.49 % and 41 % were recorded for PEP and PE respectively. Al_2O_3-PP (C-PP) separator recorded the least porosity. Al_2O_3 particles settled in the pores of the PP separator and also coated the surface of the PP separator. This significantly reduced the porosity of the C-PP separator. Fig. 2d shows that PET separators have a relatively larger pore structure as compared to the polyolefin and C-PP separators. PET separators have larger fibers that are not cross-linked. The packing of these large fibers creates a porous network of large pores in the separator membrane and accounts for the higher porosity of 49.5 % for this membrane. A unique feature is observed in the SiCmat separator as shown in Fig. 2b. SiCmat membrane combines larger and smaller fibers to form a networked membrane that holds and distributes electrolytes to facilitate quick ion transport. The advantage that this membrane provides is seen as this membrane recorded the highest porosity value of 66 %.

The composition or nature of any two materials that are in contact (in this case the electrolyte and the separator) and surface properties highly influence electrolyte adsorption and absorption. For lithium-ion batteries, the properties of electrolyte adsorption and/or absorption influence the battery's performance. Whereas adsorption positively affects battery performance, absorption may provide long-term negative feedback on the battery performance [23,24]. Adsorption increases wettability thus it improves ionic conductivity allowing for better battery performance at high C-rates [25]. Absorption on the other hand impregnates the separator material with electrolyte which leads to swelling in some separators. Swelling reduces separator porosity which ultimately decreases the cycling performance of the battery [26]. The

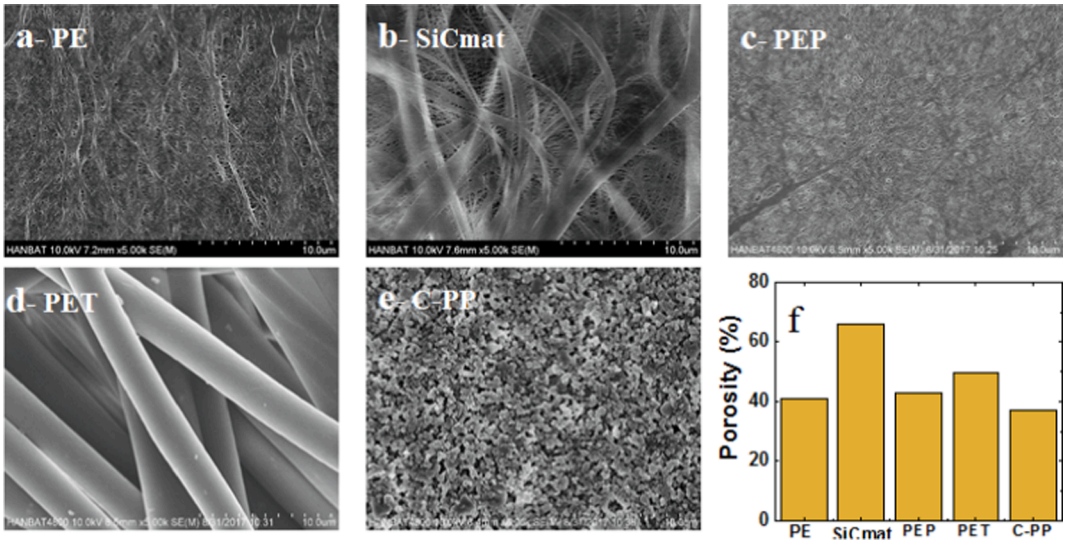

Fig. 2. FESEM images of the surfaces of a) PE b) SiCmat c) PEP d) PET e) C-PP, f) porosity value of the different separators.

contact angles formed by a drop of the electrolyte on the surfaces of the separators are provided in Fig. 3 (a-e). Hydrophobic materials have low surface energy whereas hydrophilic materials have high surface energy. The higher the surface energy of a material the higher its wettability by polar solvents [27]. The chemical structures of the different separators are depicted in Fig. 4. The electrolyte contact angle was highest for the polyolefin separators followed by the SiCmat separator then the C-PP separator and finally the PET separator. Polyolefin separators are composed of carbon-hydrogen single bonds (C–H) which are responsible for the low surface energy and the hydrophobicity of the separators. This hydrophobicity reduces the adsorption and spreading of the hydrophilic electrolyte on the surface of polyolefin separators leading to poor wetting of the separator materials by the electrolyte. Therefore the established electrolyte contact angles for PE and PEP separators were 45.21° and 43.14° respectively, which were high. Al_2O_3 has high surface energy due to the presence of polar oxygen groups. The high surface energy of Al_2O_3 allowed for the adsorption, spreading and wetting of the C-PP separator by the electrolyte hence it demonstrated an electrolyte contact angle of 10.75°. SiCmat is moderately hydrophilic and it also permits the adsorption, spreading and wetting of the electrolyte on its surface. Therefore the electrolyte contact angle recorded on the surface of SiCmat was 35.96° which is lower than the values recorded for the polyolefin separators. The electrolyte contact angle measured for PET separator was 0° as can be seen in Fig. 3d. PET polymer has abundant oxygen groups as part of the polymeric fiber structure (See Fig. 4). Due to the high number of oxygen groups, PET separators have high surface energies making them very hydrophilic. PET separators therefore adsorb and spread electrolytes on the surface quickly which promotes wettability. The ester groups (–COO-) in PET provide them with a high affinity toward polar solvents. This oxygen-rich group in PET allows for the absorption of the electrolytes into the PET separator structure by polar interactions. Electrolyte absorption by PET causes it to swell with continuous usage [28].

A blend of good porosity and high surface wettability is necessary to achieve high ionic conductivity across separator membranes. Fig. 3f provides a summary of the ionic conductivity of the electrolyte solution across the different separator membranes. The ionic conductivity

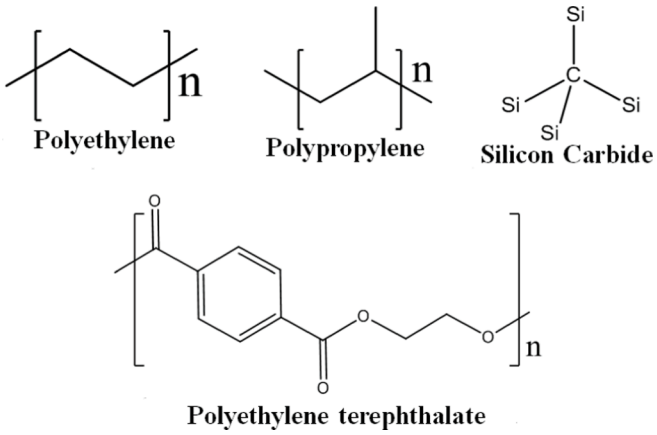

Fig. 4. The chemical structure of the various separators used in this study.

measured across the PET separator was 2.586 $mScm^{-1}$ and that measured across the SiCmat separator was 1.820 $mScm^{-1}$. PET separator with its high surface wettability and good membrane porosity makes it highly ionic conducting. Whereas SiCmat is more porous than the PET separator the latter is easily wetted by the electrolyte. This allows the PET separator to retain more electrolyte solution in its pores than the SiCmat, explaining why the ionic conductivity was higher across the PET membrane than the SiCmat separator. The ionic conductivity values recorded for the PEP separator and C-PP were 0.713 $mScm^{-1}$ and 0.960 $mScm^{-1}$ respectively. These values were less than half the value measured for the PET separator. Again both PEP separator and C-PP separator are less porous than PET and SiCmat separators. PEP separator is also less wetting than the nonwoven PET and SiCmat separators. Although coating the surface of the PP separator with alumina improves membrane wettability, it reduces membrane porosity. Therefore ionic conductivity recorded for the C-PP separator was slightly higher than the PEP separator. The ionic conductivity measured for the PE separator was 1.020 $mScm^{-1}$ and this is due to the better electrolyte wettability and uptake compared to C-PP and PEP.

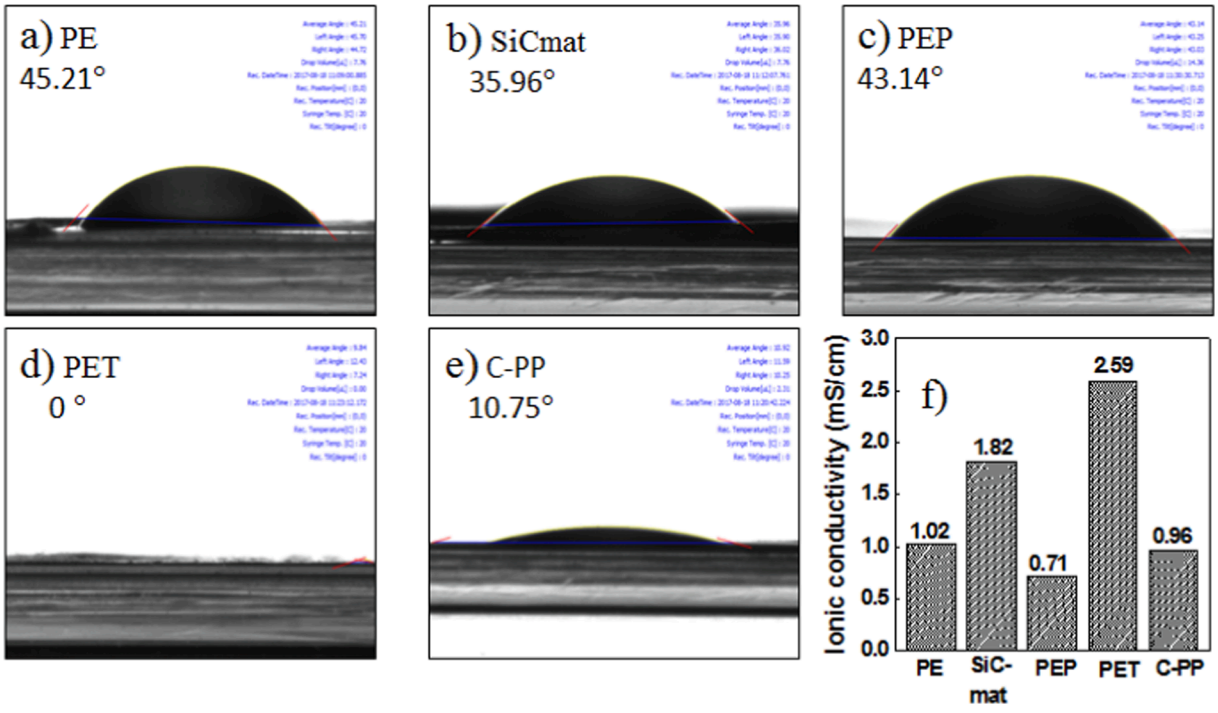

Fig. 3. Contact angle pictures of a) PE b) SiCmat c) PEP d) PET e) C-PP, f) the ionic conductivity of the different separators.

To compare the electrochemical stability of the separators the linear sweep voltammetry of the membranes was studied against lithium metal. The linear sweep voltammetry plots for the separators presented in Fig. 5 provide comparisons for the electrochemical stability of the different separators. All the separator membranes displayed good electrochemical stability; above 4.5 V. Polyolefin separators have excellent chemical stability and high mechanical strength [29]. The PE separator was the most stable while the SiCmat was the least stable. It can however be argued based on the LSV observation made that all the separators can be successfully used in combination with high voltage cathodes with minimum effect.

The effects of separator membranes on battery performance and cycle life were investigated at room temperature and different charge–discharge rates. The charge–discharge performance obtained at the different rates is provided in Fig. 6 (a-e). The good electrochemical stability of the separator membranes provided by the LSV analysis eliminates the possible contribution to poor charge–discharge performance by the separator membranes. Therefore any differences in the charge–discharge performance of the batteries can be attributed to the differences in membrane porosity and separator-electrolyte interactions (absorption, adsorption and wettability of the separator membranes). All the cells constructed with the different separators showed similar discharge capacities (150 mAh/g to 180 mAh/g) at low C-rates (0.1C to 0.5C). At high C-rates, the differences in membrane porosity, electrolyte adsorption and wettability greatly influenced the discharge capacities delivered for each separator. Discharge delivery capacities obtained for the polyolefin separators were the least (< 60 mAh/g) due to the poor ionic conductivity of the electrolyte across the polyolefin membranes. The discharge capacity of C-PP separators was greatly improved at high C-rates compared to PE and PEP as shown in Fig. 6. This may be attributed to the presence of the alumina. Alumina coated on PP separators enhanced the electrolyte adsorption and wettability of the PP membrane which allows for lithium ion transport across the membrane. Again this observation suggests that electrolyte adsorption by separator membranes greatly impacts battery performance more positively than the porosity of the membrane. The PET and SiCmat separators showed similar capacities at both high and low C-rates. Both separators delivered the highest capacities compared to the others (> 87 mAh/g and > 130 mAh/g at 10C and 5C discharges respectively) due to the combination of good membrane porosity and electrolyte wettability in SiCmat and PET membranes as shown in the charge–discharge graphs for SiCmat and PET separators in Fig. 6a and Fig. 6d respectively.

Fig. 7a displays the EIS of the cells assembled using the different separators before the cycle performance test at room temperature. The inset describes the corresponding equivalent circuit fitting for the impedance measurement. The Nyquist plots in both the high and medium frequency regions are characterized by semicircles that represent the sum of the charge transfer resistance across the cells. The Warburg impedance (straight line portion) seen in the low-frequency region of the Nyquist plot describes the lithium-ion diffusion process across the separator membranes [30]. The first recorded value is interpreted as the bulk cell resistance while the smaller semicircle in the high-frequency region is associated with the establishment of the Solid Electrolyte Interface (SEI). All the separators showed slight differences in their charge transfer resistance. Cells assembled with PET, PE, and PEP separators show the least charge transfer resistance values of 42.007 Ωcm, 44.656 Ωcm and 45.658 Ωcm due to the establishment of a good SEI layer in these cells. The good SEI promoted the transport of lithium ions across the membranes. In the case of C-PP and SiCmat separators, the charge transfer resistances recorded were 49.804 Ωcm and 46.605 Ωcm implying that the SEI formed were slightly poor performing. A summary of the resistance values extracted from the plots is provided in Table 2.

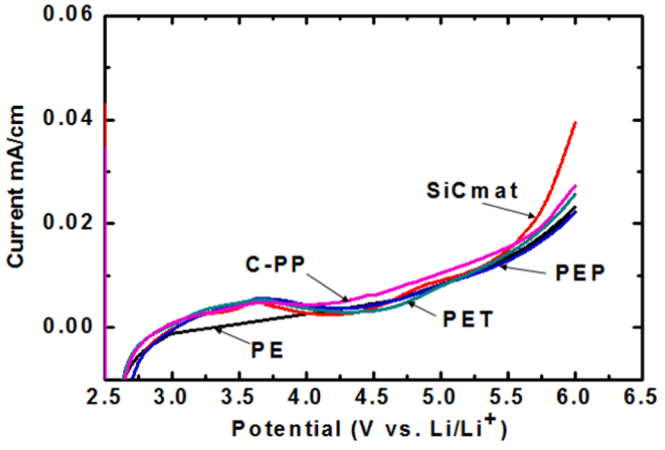

Fig. 5. Linear sweep voltammogram of the different separators using electrolyte consisting of 1 M $LiPF_6$ (EC/DMC = 3:7) at rate of 0.1 m/s and a potential range of 2.5–6 V.

Fig. 7b shows the life cycle performance of the different separator membranes at 1C and room temperature. The first cycle discharge capacities are very high for all the separators (>150 mAh/g), showing a similar cycling trend. Using the second discharge capacity to compute the capacity retention of the cells employing the different separators, it was observed that all the cells were fairly stable with the different separators. The capacity retention is in the order of C-PP < PE < PEP < SiCmat < PET corresponding to 85 %, 88.3 %, 88.5 %, 88.6 % and 88.9 % respectively after the 100th cycle. The nonwoven separators showed higher capacity retention compared to the polyolefin separators. This may be attributed to the high electrolyte uptake and hence the low solution resistance observed in the Nyquist plot (See Table 1 and Table 2). The SiCmat separator showed a second discharge capacity of 123.2 mAh/g and ended with 109.5 mAh/g. The cell with PET separator started with 131 mAh/g and ended with a capacity of 117 mAh/g. The PE separator started with a specific capacity of 137 mAh/g, ending with a specific capacity of 121 mAh/g after the 100th cycle. The PEP separator recorded an initial capacity of 137 mAh/g and recorded a capacity of 120 mAh/g after the 100th cycle. Lastly, the C-PP recorded the least with an initial capacity of 130 mAh/g and recorded a specific capacity of 110 mAh/g after the 100th cycle. Generally, all the LIB cells employing the different separators showed good capacity retention after the 100th cycle.

Separators are known to prolong self-discharge time which improves battery capacity [31]. They are also advantageous in shutting down redox channels that may form due to short circuits. In such events, the batteries are protected from fires which may lead to battery ignition. Thermo gravimetric analysis (TGA) experiments were done to evaluate the stability of the separator membranes at high temperatures. Fig. 8a shows the thermal shrinkage property of the graphs provided by TGA. As seen from the TGA graph polyolefin separators have high thermal shrinkages. This characteristic of polyolefin separators may trigger fires because of internal shorts which make batteries unsafe for use at high temperatures and high C-rate discharge conditions. However, coating the PP separator with alumina (more heat tolerant) helps to improve the thermal stability of the PP membrane. PET separators shrunk less due to the high thermal stability of the aromatic constituent of the polymer fiber. The SiCmat also showed less thermal shrinkage than the polyolefin separators. Silicon carbide exhibits intrinsic properties such as high tensile strength, high elastic modulus, excellent thermal stability and excellent oxidation resistance [32]. The thermal shrinkage images of the separators performed at 140 °C for two hours are provided in Fig. 8b. The observation made from this test also supports the thermal stability trend found in the TGA.

4. Conclusion

The influences of PE, SiCmat, PEP, PET and C-PP separator materials on the electrochemical performance of $LiNi_{1/3}Mn_{1/3}Co_{1/3}O_2$ (NMC-333)

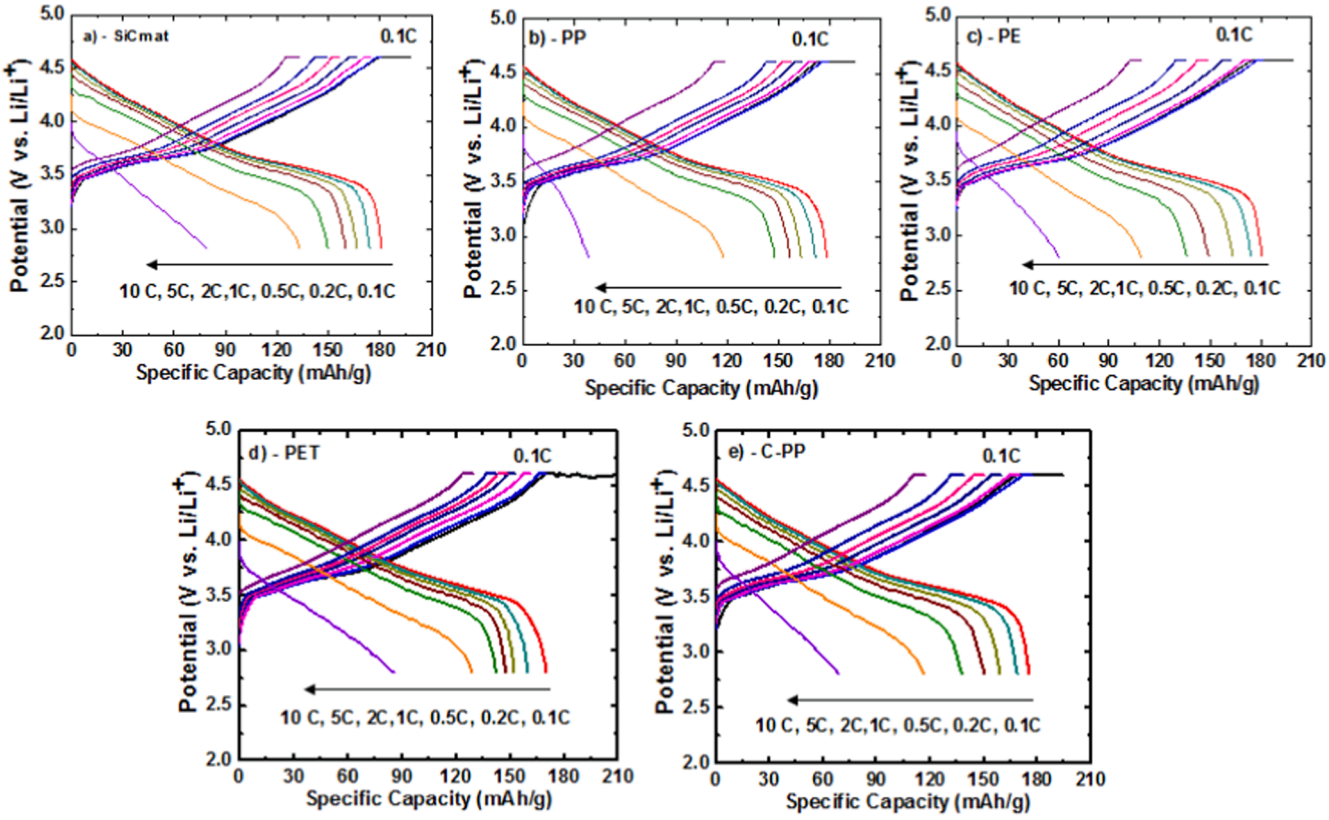

Fig. 6. Charge-discharge curves of NMC-333/graphite cell with the different separator from 2.8 −4.6 V at different scan rate.

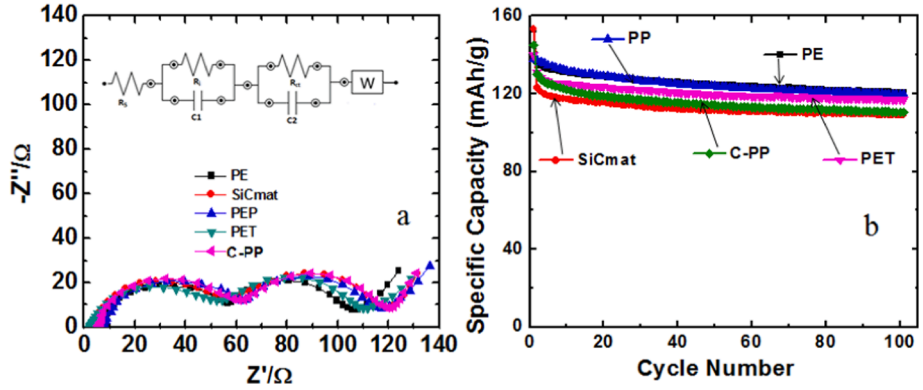

Fig. 7. A) Nyquist plot of the NMC-333/graphite cell with the different separator before charge–discharge cycle b) Cycle performance of the NMC-333/graphite cell with the different separator.

Table 1
Physical properties of the different separators.

Separator	Thickness / (μm)	Electrolyte uptake / (%)	Ionic conductivity / (mScm-1)
PE	20	120	1.020
SiCmat	43	150	1.820
PEP	19	92	0.713
PET	36	195	2.586
C-PP	16	112	0.960

cathode were investigated at room temperature. Electrolyte adsorption, wettability, and membrane porosity impact ionic conductivity. However, electrolyte adsorption and wettability affect the ionic conductivity and high C-rate performance of lithium-ion batteries more than the membrane porosity does. For selectivity based on thermal performance

Table 2
Internal resistance characteristics of NMC-333/graphite cell with the different separator.

Separator	Solution Resistance (R_S) / (Ωcm)	Resistance of SEI layer (R_{SEI}) / (Ωcm)	Charge Transfer Resistance (R_{CT}) /(Ωcm)	Warburg Impedance (R_W (Ω)
PE	6.630	45.795	44.656	0.108
SiCmat	3.181	56.287	46.605	0.104
PEP	7.641	48.263	45.658	0.109
PET	2.341	53.394	42.007	0.096
C-PP	5.303	53.603	49.804	0.110

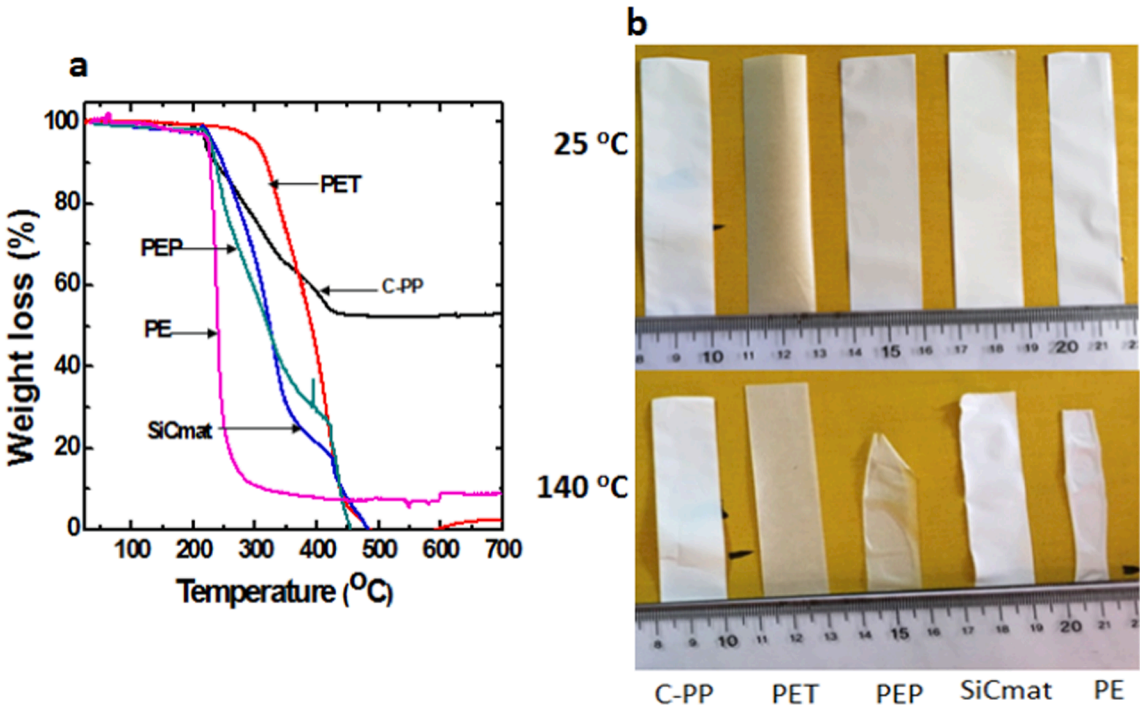

Fig. 8. A) photographs of the separators after heating at 25 °C and 140 °C for 60 min (b) Thermo gravimetric analysis of the different separators.

or cycle stability, there will be the need for trade-offs to achieve maximum and superior performance based on desired performance. The capacity retention of the different separators is in the order of C-PP < PE < PEP < SiCmat < PET with corresponding values of 85 %, 88.3 %, 88.5 %, 88.6 % and 88.9 %, implying that the nonwoven separators worked synergistically with the liquid electrolyte to maintain stable cycle performance over the 100 charge–discharge cycle. C-PP, PET and SiCmat are reliable separators for applications that require good thermal stability. In addition, PET and SiCmat also provided good cycling performance thus making them suitable alternatives to the commercially available PE or PEP.

CRediT authorship contribution statement

Louis Hamenu: Writing – review & editing, Writing – original draft, Methodology, Investigation, Formal analysis, Data curation, Conceptualization. **Latifatu Mohammed:** . **Juliet Attah:** Writing – review & editing, Investigation. **Rafia Abdul-Samii:** Investigation, Data curation. **Eric Nyarko:** Resources. **Anna Monney Hammond:** Resources, Data curation. **Godfred Ofotsu Tottimeh:** . **Joyce Koranteng:** Software, Resources. **Kennedy Andoh:** Software, Resources. **Alfred Madzvamuse:** Writing – review & editing.

Declaration of competing interest

The authors declare that they have no known competing financial interests or personal relationships that could have appeared to influence the work reported in this paper.

Data availability

Data will be made available on request.

Acknowledgement

The research team would like to acknowledge the applied electrochemistry laboratory at Hanbat National University, Daejeon, South Korea for supporting this work.

References

[1] J.B. Goodenough, K.-S. Park, The Li-ion rechargeable battery: a perspective, Journal of American Chemical Society 135 (4) (2013) 1167–1176.
[2] D. Mohanty, J. Li, R. Born, L.C. Maxey, R.B. Dinwiddie, C. Daniel, D.L. Wood III, Non-destructive evaluation of slot-die-coated lithium secondary battery electrodes by in-line laser caliper and IR thermography methods, Analytical Methods 6 (3) (2014) 674.
[3] M. Bharathidasan, V. Indragandhi, V. Suresh, M. Jasiński, Z. Leonowicz, A review on electric vehicle: Technologies, energy trading, and cyber security, Energy Report 8 (2022) 9662–9685.
[4] W. Liu, T. Placke, K.T. Chau, Overview of batteries and battery management for electric vehicles, Energy Report 8 (2022) 4058–4084.
[5] Y. Lyu, Y. Liu, Z.-E. Yu, N. Su, Y. Liu, W. Li, Q. Li, B. Guo, B. Liu, Recent advances in energy-density cathode materials for sodium-ion battery, Sustainable Materials and Technologies 21 (2019) e00098.
[6] D. Andre, S.-J. Kim, P. Lamp, S.F. Lux, F. Maglia, O. Paschos, B. Stiaszny, Future Generations of Cathode Materials: An Automotive Industry Perspective, Journal of Materials Chemistry A, 3 (13) (2015) 6709–6732.
[7] M. Akhilash, P.S. Salini, Bibin John, T.D. Mercy, A journey through layered cathode materials for lithium ion cells – From lithium cobalt oxide to lithium-rich transition metal oxides, Journal of Alloys and Compounds 869 (2021) 159239.
[8] M. Latifatu, C.Y. Bon, K.S. Lee, L. Hamenu, Y.I. Kim, Y.J. Lee, Y.M. Lee, J.M. Ko, Structural Effect of Conductive Carbons on the Adhesion and Electrochemical Behavior of LiNi0.4Mn0.4Co0.2O2 Cathode for Lithium Ion Batteries, *Journal of electrochemistry Science and Technology*, 9, 4 (2018) 330-338 .
[9] M. Latifatu, M. Hu, S.J. Kim, C.Y. Bon, C. Kang, W.I. Cho, J.M. Ko, Mengyang Hu, Sang Jun Kim, Chris Yeajoon Bon, Chiwon Kang, Won Il Cho, Jang Myoun Ko, Lithium modified silica as electrolyte additive for lithium secondary batteries, Solid State Ionics 319 (2018) 7–12.
[10] P. Zhao, J. Yang, Y. Shang, L.i. Wang, M. Fang, J. Wang, X. He, Surface modification of polyolefin separators for lithium ion batteries to reduce thermal shrinkage without thickness increase, *Journal of Energy*, Chemistry 24 (2) (2015) 138–144.
[11] M. Liu, P. Zhang, L. Gou, Z. Hou, B. Huang, Enhancement on the thermostability and wettability of lithium-ion batteries separator via surface chemical modification, Material Letters 208 (2017) 98–101.
[12] X. Jiang, X. Zhu, X. Ai, H. Yang, Y. Cao, Novel ceramic-grafted separator with highly thermal stability for safe lithium-ion batteries, ACS Applied Materials & Interfaces 9 (2017) 25970–25975.
[13] R. Laurita, M. Zaccaria, M. Gherardi, D. Fabiani, A. Merlettini, A. Pollicino, M. L. Focarete, V. Colombo, Plasma processing of electrospun Li-ion battery separators to improve electrolyte uptake, *Plasma Processing*, Polymer 13 (1) (2016) 124–133.
[14] L. Mohammed, B. Boating, M. Mwemez, L. Hamenu, A. Madzvamuse, A. Nyarko, M. Mohammed, W. Oduro, F.B. Agyenim, Y.M. Lee, J.M. Ko, EMI-BF_4 electrolyte and Al_2O_3/PVDF-HFP modified PE separator for high capacitance retention and

cycle stability in supercapacitors, *The Korean Institute of Chemical Engineering* 39 (2022) 3003–3301.
[15] K. Kwang Man, L. Mohammed, L. Young-Gi, K. Jang Myoun, K. Jong Huy, C. Won II, Effect of ceramic filler-containing polymer hydrogel electrolytes coated on polyolefin separator on the electrochemical properties of activated carbon supercapacitor, Journal of Electroceramics 32 (2014) 146–153, https://doi.org/10.1007/s10832-013-9860-6.
[16] C.Y. Bon, L. Mohammed, S. Kim, M. Manasi, P. Isheunesu, K.S. Lee, J.M. Ko, Flexible poly (vinyl alcohol)-ceramic composite separators for supercapacitor applications, Journal of Industrial and Engineering Chemistry 68 (2018) 173–179, https://doi.org/10.1016/j.jiec.2018.07.043.
[17] R.R. Bresee, U.A. Qureshi, M.C. Pelham, Influence of processing conditions on melt blown web structure: Part 2–Primary airflow rate 14 (2005) 11–18.
[18] N.K. Amogh, J.B. Troy, A.D. Virginia, J.T. Bruce, A novel nano-nonwoven fabric with three-dimensionally dispersed nanofibers: entrapment of carbon nanofibers within nonwovens using the wet-lay process, Nanotechnology 23 (2012), 185601, https://doi.org/10.1088/0957-4484/23/18/185601.
[19] J. Veitl, H.-K. Weber, M. Frankenberger, K.-H. Pettinger, Modification of Battery Separators via Electrospinning to Enable Lamination in Cell Assembly, Energies 15 (22) (2022) 8430.
[20] M. Stephen, P. Behnam, D. Prashant, Review of thermally point-bonded nonwovens: materials, processes, and properties, Journal of Applied Polymer Science 99 (2006) 2489–2496.
[21] Carlos M. Costa, Yong-Hyeok Lee, Jung-Hwan Kim, Sang-Young Lee, Senentxu Lanceros-Mendez, Recent advances on separator membranes for lithium-ion battery applications: From porous membranes to solid electrolytes, Energy Storage Materials 22 (2019) 346–375.
[22] H.-G. Wang, S. Yuan, D.-L. Ma, X.-B. Zhang, J.-M. Yan, Electrospun materials for lithium and sodium rechargeable batteries: from structure evolution to electrochemical performance, Energy & Environmental Science 8 (2015) 1660–1681.
[23] F. Liu, X. Chuan, Recent developments in natural mineral-based separators for lithium-ion batteries, RSC Advances 11 (27) (2021) 16633–16644.
[24] Y. Li, Q. Li, Z. Tan, A review of electrospun nanofiber-based separators for rechargeable lithium-ion batteries, Journal of Power Sources 443 (2019), 227262.
[25] C.M. Costa, Y.-H. Lee, J.-H. Kim, S.-Y. Lee, S. Lanceros-Méndez, Recent advances on separator membranes for lithium-ion battery applications: From porous membranes to solid electrolytes, Energy Storage Materials 22 (2019) 346–375.
[26] G.Y. Gor, J. Cannarella, C.Z. Leng, A. Vishnyakov, C.B. Arnold, Swelling and softening of lithium-ion battery separators in electrolyte solvents, Journal of Power Sources J. Power Sources 294 (2015) 167e172.
[27] Seyedabbas Rasouli, Nima Rezaei, Hamideh Hamedi, Sohrab Zendehboudi, Xili Duan, Superhydrophobic and superoleophilic membranes for oil-water separation application: A comprehensive review, Materials & Design 204 (2021) 109599.
[28] Y. Zhang, L. Ying, Z. Wang, Y. Wang, Q. Xu, C. Li, Unexpected hydrophobic to hydrophilic transition of PET fabric treated in a deep eutectic solvent of choline chloride and oxalic acid, Polymer 234 (8) (2021), 124246.
[29] A.A. Heidari, H. Mahdavi, Recent Development of Polyolefin-Based Microporous Separators for Li-Ion Batteries: A Review, The Chemical Record 20 (6) (2020) 570–595.
[30] R. Weber, A. J. Louli, K. P. Plucknett, J. R. Dahn, Resistance Growth in Lithium-Ion Pouch Cells with LiNi0.80Co0.15Al0.05O2 Positive Electrodes and Proposed Mechanism for Voltage Dependent Charge-Transfer Resistance, Journal of the Electrochemical Society, 166, 10 (2019) A1779-A1784.
[31] S. Zhong, B. Yuan, Z. Guang, D. Chen, Q. Li, L. Dong, Y. Ji, Y. Dong, J. Han, W. He, Recent progress in thin separators for upgraded lithium ion batteries, Energy Storage Materials 41 (2021) 805–841.
[32] P.-H. Kang, J.-P. Jeun, D.-K. Seo, Y.-C. Nho, Fabrication of SiC mat by radiation processing, Radiation Physics and Chemistry 78 (7–8) (2009) 493–495.